IMPROVED LINEAR AXISYMMETRIC SHELL-FLUID MODEL FOR LAUNCH VEHICLE LONGITUDINAL RESPONSE ANALYSIS*

J. S. Archer**
C. P. Rubin***

TRW Systems
Redondo Beach, California

An improved linear analytical model is developed for the calculation of axisymmetric launch vehicle longitudinal vibration modes and steady-state response to applied axisymmetric harmonic loads. This approach utilizes a finite element technique to construct the total vehicle stiffness and mass matrices by subdividing the structure into a set of (1) axisymmetric shell components (2) fluid components and (3) spring-mass components. The total vehicle characteristics are obtained by superposition of the stiffness and mass matrices of the individual shell, fluid and spring-mass components. General expressions for the stiffness and mass matrices of conical and ellipsoidal shells of revolution are derived taking into account the initial stresses. The fluid mass matrix is derived using fluid motions which are consistent with the shell component distortions. The natural frequency solution of a typical launch vehicle configuration is presented for illustration and contrasted with the results obtained from a lumped spring-mass model.

NOTATION****

$a1$, $a2$, $a3$	Identification numbers for the shell components which enclose a fluid component
$[A]_{(\bar{U}\times 11)} \equiv [a_{kn}]$	Polynomial matrix associated with $u_k(\xi)$
$[B]_{(\bar{V}\times 11)}$ $[b_{\ell n}]$	Polynomial matrix associated with $v_\ell(\xi)$
C_{11}, C_{12}, C_{22}	Orthotropic stress-strain coefficients
C_{33}, C_{34}, C_{44}	Orthotropic moment-curvature coefficients
$[D_1]_{(2\times 11)}$, $[D_2]_{(2\times 11)}$	Matrices used in the definition of the rotation vector $\{\rho\}$
e	General identification number for vehicle components which may stand for a or b
H	Total fluid level measured positive upward from the base of a2
$[K]_{(N_c \times N_c)}$	Total launch vehicle stiffness matrix

*This work was performed under NASA Contract NAS-1-4351.

**Manager, Dynamics Department
***Member of Technical Staff

****Only quantities which appear more than once or are undefined in the text are included in the Notation Section.

K_a	Stiffness matrix for shell component a associated with the system coordinates
$[\bar{K}_a]_{((\bar{U}+\bar{V})\times(\bar{U}+\bar{V}))}$	Stiffness matrix for shell component a associated with the local coordinates
K_c	Stiffness matrix of spring-mass component c associated with the system coordinates
K_ϕ, K_θ	Shell meridional and hoop curvatures, respectively
L	Length of conical shell
L_{a3}	Height of shell a3
$[M]_{(N_c \times N_c)}$	Total mass matrix for the launch vehicle
M_a	Mass matrix for shell component a associated with the system coordinates
$[\bar{M}_a]_{((\bar{U}+\bar{V})\times(\bar{U}+\bar{V}))}$	Mass matrix for shell component a associated with the local coordinates
M_b	Mass matrix for fluid component b associated with the system coordinates
$[\bar{M}_b]_{(\bar{W}\times\bar{W})}$	Mass matrix for fluid component b associated with the local coordinates
M_c	Mass matrix for spring-mass component c associated with the system coordinates
N_C	Total number of system coordinates used in the vehicle model
N_ϕ^o	Initial meridional stress
p	Circular frequency of the vehicle
P	Applied load vector
r	Radial distance from the vehicle longitudinal axis to each point on the shell
$\hat{r}$	Radial distance from the vehicle longitudinal axis to each point in the fluid
r_1	Meridional radius of curvature of the shell
t	Time
$[T_a]_{((\bar{U}+\bar{V})\times(\bar{U}+\bar{V}))}$	Transformation matrix which relates local to system coordinates in shell component a
$[T_b]_{(\bar{W}\times\bar{W})}$	Transformation matrix which relates local to system coordinates in fluid component b
$\{U\}_{((U+V)\times 1)}$, $\{V\}_{((U+V)\times 1)}$	Longitudinal and radial displacement vectors, respectively, for shell components
$u_k(\xi)$, $v_\ell(\xi)$	Generalized longitudinal and radial displacements, respectively, for shell components
$\{\hat{U}(x)\}_{(\bar{W}\times 1)} = \{\hat{U}_m(x)\}$ and $\{v(\hat{x},\hat{r})\}_{(\bar{W}\times 1)} = \{\hat{v}_m(x,\hat{r})\}$	Longitudinal and radial fluid displacements, respectively where $1 \le m \le \bar{W}$

U, V Total number of longitudinal and radial system coordinates, respectively, associated with each shell component

$\overline{U}, \overline{V}$ Total number of longitudinal and radial local coordinates, respectively, associated with each shell component

$[U]_{(U \times 1)}, [V]_{(V \times 1)}$ Constant matrices used in the definition of the system coordinates

$\overline{W}$ The sum of $\overline{U} + \overline{V}$ for the three shells surrounding a fluid component

x Longitudinal axis of the launch vehicle

$\{a_a\}_{((\overline{U}+\overline{V}) \times 1)}$ Modal vector whose components are the longitudinal, radial and rotational system coordinate displacements for shell component a

$\{\overline{a}_a\}_{((\overline{U}+\overline{V}) \times 1)}$ Consolidated vector of local coordinates

$\{\overline{a}_k\}_{(\overline{U} \times 1)}, \{\overline{\beta}_\ell\}_{(\overline{V} \times 1)}$ Generalized coordinates in the longitudinal and radial directions, respectively

γ_a, γ_b Mass densities for shell and fluid components respectively

Δ_e Transformation matrix relating total system displacements to component system displacements

$\epsilon_\phi, \epsilon_\theta$ Meridional and hoop strains, respectively, ror the shell components

ξ Nondimensional variable describing location on each shell component

ρ Meridional rotation of the shell components

ϕ Meridional angle

1.0 INTRODUCTION

This paper describes an improved linear analytical model developed for the calculation of axisymmetric launch vehicle longitudinal vibration modes and steady-state response to applied axisymmetric harmonic loads. The detailed equations which have been coded in Fortran IV for digital computer solution are contained in Reference 1. Reference 2 is the detailed computer programming manual for the digital program. The work discussed here was accomplished under contract to the NASA Langley Research Center.

In the evaluation of launch vehicle behavior, it is necessary to study the response of the entire vehicle to a wide variety of dynamic loadings to insure the structural integrity and stability of the system. As a result, much effort has gone into the development of techniques to calculate the vehicle response to lateral and longitudinal loadings using distributed and lumped spring-mass models and techniques for the theoretical and empirical modeling of the vehicle behavior. Reference 3, for example, discusses the technique of generating a lumped mass-spring model for representing the longitudinal dynamic characteristics of liquid propellant boosters with particular emphasis on the method of handling the fluid masses. The technique is applicable to cylindrical tanks with flexible lower bulkheads and to semimonocoque cylinders with partially buckled skins. Experimental data, however, indicates that lumped mass-spring models, including the one discussed in Reference 3, are unsatisfactory in several respects. Among other things, accurate representation of important structural shell characteristics and realistic coupling of the fluids with the detailed structural behavior of tank walls and bulkheads are omitted.

The approach described herein overcomes to a large extent the above noted deficiencies. A finite element technique is utilized to construct the total launch vehicle stiffness matrix **K** and mass matrix **M** by subdividing the prototype structure into a set of (1) axisymmetric shell components, (2) fluid components, and (3) spring-mass components. In this way, it is possible to represent as separate shell units the fairing, interstage structure, bulkheads, tank walls and engine thrust structure, and to conveniently provide for the inertial and stiffness characteristics of equipment, engines and vehicle supporting structure. Fluid motions are accounted for in a manner consistent with the shell component distortions, neglecting free surface effects.

The stiffness and mass matrices for the complete launch vehicle are obtained by superposition of the stiffness and mass matrices of the individual shell, fluid and spring-mass components which are computed using a Rayleigh-Ritz approach. The superposition technique assures displacement compatibility and force ecuilibrium at the interfaces between components. After the complete system stiffness and mass matrices have been formulated, displacement boundary conditions are introduced by removing appropriate rows and columns corresponding to points on the vehicle and its supports which are rigidly restrained from motion.

The coupled system's natural frequencies and mode shapes are obtained from the eigenvalue equation constructed with the total stiffness and mass matrices

$$[K]\{a\} - p^2[M]\{a\} = 0 \qquad (1)$$

in which p is the circular frequency of the system and $\{a\}$ is the modal vector whose components are the longitudinal, radial and rotational displacements at discrete points on the vehicle. The steady-state response due to simple harmonic loads is determined using a standard modal response procedure which expresses the total displacement, velocity, acceleration and force responses as the linear superposition of the individual modal responses based on an assumed modal damping.

The procedure will handle shell components with a wide range of geometries. It includes shell effects in the tank and bulkhead structure, but avoids the need for including detailed local deformation, such as at shell discontinuities, which are unimportant in determining the total dynamic behavior of the vehicle. The approach has the capability of representing the tank or stage of most interest in great detail and those of least interest with minimum detail, as desired, thereby minimizing the computation time required and remaining within the maximum limitations of standard eigenvalue routines. The formulation of the problem is subdivided into well-defined portions, leading to efficient coding and easy modification for later incorporation of asymmetric shell behavior and even more detailed treatment of the fluid behavior.

2.0 ANALYTICAL MODEL

As illustrated in Figure 1, the launch vehicle structure is subdivided into a consistent set of shell components, fluid components and multicoordinate spring-mass components. In the present approach the stiffness and mass characteristics of each of the shell components is then computed using the Rayleigh-Ritz technique. This calculation is based on an assumed displacement pattern having a polynomial representation. These displacement functions, associated with the individual shell components, are designated as local coordinate displacements.

The mass matrix for each fluid component is also computed by a Rayleigh-Ritz approach but in this case the fluid motions are not arbitrarily specified but are derived assuming transverse plane surfaces remain plane and by satisfying continuity and the conditions of compatibility at the tank wall interface. The fluid motions therefore take into account the geometric coupling of the fluid to the shell components.

In order to have a convenient method of combining the individual stiffness and mass matrices to obtain the total system matrices, a coordinate system common to all components is introduced and is designated as system coordinates. These coordinates represent longitudinal and radial translations and the rotation about specific parallels on the axisymmetric vehicle structure. The controlling parallels or stations whose motion is represented by the system coordinates are located at the intersections between shell components, at equally spaced intermediate parallels on a shell component, at intersections of the longitudinal axis with a shell component and on lumped masses as illustrated in Figure 1b.

By a suitable transformation the stiffness and mass matrices in terms of local coordinates are transformed into matrices which are related to the system coordinates. These matrices are superimposed to form the total system stiffness and mass characteristics.

Due to limitations on the storage capacity of the IBM 7094 digital computer, a number of restrictions were placed on the present analysis. The total vehicle which may be represented is limited to one with not more than six fluid components. The total number of shell components may not exceed forty. The characteristics of the spring-mass components representing such equipment as engines and mass-elastic supports are provided directly by low order (≤ 10) stiffness and mass matrices. The total number of spring-mass components may not exceed thirty. The number of non-fixed degrees-of-freedom by which the behavior of the system is described may not exceed eighty.

The specific shell components to be used are conical frustums (which include cylindrical shells as a special case) and ellipsoidal bulkheads (which include hemispherical shells as a special case). Within the domain of thin shell theory, the shell components may have orthotropic properties and a linear thickness variation in the meridional direction. Local thickening of a shell at a bulkhead or wall joint may be handled by using an equivalent local hoop stiffener which is provided as input in the form of an additional spring-mass component. Initial static stresses based on membrane theory are accounted for in determining the stiffness matrix for the shell components.

The most general fluid component may be in contact with an ellipsoidal upper bulkhead, a conical tank wall, and a conical or ellipsoidal lower bulkhead. The bulkhead shell elements may be convex down or up with fluid at any desired depth on either side, both sides or neither side.

3.0 SHELL STIFFNESS AND MASS MATRICES

As described in the previous section, the governing equations for the individual shell and fluid components are first derived in terms of generalized coordinate displacements (local coordinates). Since each shell of revolution is subjected to only axisymmetric loads, its behavior may be expressed in terms of two displacement components, u and v (see Figure 2). In the usual Rayleigh-Ritz manner these displacements will be represented by a finite series having the form

$$u(\xi) = \sum_{k=1}^{\overline{U}} \overline{\alpha}_k u_k(\xi) , \quad \overline{U} \leq 11$$

$$v(\xi) = \sum_{\ell=1}^{\overline{V}} \overline{\beta}_\ell v_\ell(\xi) , \quad \overline{V} \leq 11 \qquad (2)$$

in which ξ is a dimensionless variable and $0 \leq \xi \leq 1$.

For the shell configurations considered in this analysis ξ is defined by

$$\xi = \frac{s}{L} \sin\phi_o \text{ for conical frustums (Figure 3)}$$
$$= \frac{\phi}{\phi_o} \text{ for convex upward ellipsoids (Figure 4)} \quad (3)$$
$$= \frac{\pi - \phi}{\pi - \phi_o} \text{ for convex downward ellipsoids}$$

The assumed mode shapes $u_k(\xi)$ and $v_k(\xi)$ consist of polynomial terms sufficient to represent all modes of shell distortion, including longitudinal stretching, radial dilation and rigid body displacements. The specific shape of the assumed modes is determined within the limitations of a tenth order polynomial, as follows:

$$u_k(\xi) = \sum_{n=0}^{10} a_{kn}\xi^n$$
$$(4)$$
$$v_\ell(\xi) = \sum_{n=0}^{10} b_{\ell n}\xi^n$$

in which $[a_{kn}] = [A](\bar{U}x11)$ and $[b_{\ell n}] = [B](\bar{V}x11)$ define the polynomial functions associated with the local coordinates $\bar{\alpha}_k$ and $\bar{\beta}_\ell$, respectively. The matrices **A** and **B** are prescribed thus permitting maximum flexibility in the selection of the assumed coordinate functions.

An energy approach is used to derive the shell stiffness and mass matrices. The additional potential energy of a shell of revolution due to distortion under axisymmetric loadings is given in the form (Reference 4)

$$V = \frac{1}{2}\int_s 2\pi r\left(N_\phi\epsilon_\phi + N_\theta\epsilon_\theta + M_\phi K_\phi + M_\theta K_\theta + N_\phi^o\rho^2\right) r_1 d\theta \quad (5)$$

in which the last term represents the work done by the initial meridional stress, N_ϕ^o. The initial hoop stress does not make a similar contribution to the potential energy since there is zero rotation in the hoop direction. In the notation of Flügge (Reference 5), the strains ($\epsilon\phi$, $\epsilon\theta$), curvatures ($K\phi$, $K\theta$) and the meridional rotation ρ are expressed in terms of the displacements $\bar{v}$ and $\bar{w}$ (see Figure 2) as follows:

$$\epsilon_\phi = \frac{1}{r_1}\left(\frac{d\bar{v}}{d\phi} + \bar{w}\right) \quad (6)$$

$$\epsilon_\theta = \frac{1}{r_2}(\bar{v}\cot\phi + \bar{w}) \quad (7)$$

$$K_\phi = \frac{1}{r_1}\frac{d}{d\phi}\left[\frac{1}{r_1}\left(\frac{d\bar{w}}{d\phi} - \bar{v}\right)\right] \quad (8)$$

$$K_\theta = \frac{\cot\phi}{r_2}\left[\frac{1}{r_1}\left(\frac{d\bar{w}}{d\phi} - \bar{v}\right)\right] \tag{9}$$

$$\rho = \frac{1}{r_1}\left(\frac{d\bar{w}}{d\phi} - \bar{v}\right) \tag{10}$$

where r_1 and r_2 are the radii of curvature of the shell in the meridional and hoop directions, respectively. Hooke's law for an orthotropic shell with the principal directions in the hoop and meridional directions takes the form: (Reference 6)

$$\begin{aligned} N_\phi &= C_{11}\epsilon_\phi + C_{12}\epsilon_\theta \\ N_\theta &= C_{12}\epsilon_\phi + C_{22}\epsilon_\theta \\ M_\phi &= C_{33}K_\phi + C_{34}K_\theta \\ M_\theta &= C_{34}K_\phi + C_{44}K_\theta \end{aligned} \tag{11}$$

The displacements u and v which are used throughout this analysis are related to Flügge's displacements by

$$\begin{aligned} \bar{v} &= -u\sin\phi + v\cos\phi \\ \bar{w} &= u\cos\phi + v\sin\phi \end{aligned}$$

Substitution of this transformation into the strains, curvature, and rotation yields

$$\epsilon_\phi = \frac{1}{r_1}\left(-\frac{du}{d\phi}\sin\phi + \frac{dv}{d\phi}\cos\phi\right) \tag{12}$$

$$\epsilon_\theta = \frac{v}{r} \tag{13}$$

$$K_\phi = \frac{1}{r_1}\frac{d}{d\phi}\left[\frac{1}{r_1}\left(\frac{du}{d\phi}\cos\phi + \frac{dv}{d\phi}\sin\phi\right)\right] \tag{14}$$

$$K_\theta = \frac{\cos\phi}{r}\left[\frac{1}{r_1}\left(\frac{du}{d\phi}\cos\phi + \frac{dv}{d\phi}\sin\phi\right)\right] \tag{15}$$

$$\rho = \frac{1}{r_1}\left(\frac{du}{d\phi}\cos\phi + \frac{dv}{d\phi}\sin\phi\right) \tag{16}$$

The stiffness matrix of each shell component is obtained by substituting the series approximation for the displacements Equations 2 to 4 into Equation 5 using Equations 11 to 16 and then performing the following differentiations:

$$\left[\overline{K}_a\right]_{((\overline{U}+\overline{V})\times(\overline{U}+\overline{V}))} = \left[\begin{array}{ccc|ccc} \frac{\partial^2 V}{\partial\overline{\alpha}_1\partial\overline{\alpha}_1} & \cdots & \frac{\partial^2 V}{\partial\overline{\alpha}_1\partial\overline{\alpha}_{\overline{U}}} & \frac{\partial^2 V}{\partial\overline{\alpha}_1\partial\overline{\beta}_1} & \cdots & \frac{\partial^2 V}{\partial\overline{\alpha}_1\partial\overline{\beta}_{\overline{V}}} \\ \vdots & & \vdots & \vdots & & \vdots \\ \frac{\partial^2 V}{\partial\overline{\alpha}_{\overline{U}}\partial\overline{\alpha}_1} & \cdots & \frac{\partial^2 V}{\partial\overline{\alpha}_{\overline{U}}\partial\overline{\alpha}_{\overline{U}}} & \frac{\partial^2 V}{\partial\overline{\alpha}_{\overline{U}}\partial\overline{\beta}_1} & \cdots & \frac{\partial^2 V}{\partial\overline{\alpha}_{\overline{U}}\partial\overline{\beta}_{\overline{V}}} \\ \hline \frac{\partial^2 V}{\partial\overline{\beta}_1\partial\overline{\alpha}_1} & \cdots & \frac{\partial^2 V}{\partial\overline{\beta}_1\partial\overline{\alpha}_{\overline{U}}} & \frac{\partial^2 V}{\partial\overline{\beta}_1\partial\overline{\beta}_1} & \cdots & \frac{\partial^2 V}{\partial\overline{\beta}_1\partial\overline{\beta}_{\overline{V}}} \\ \vdots & & \vdots & \vdots & & \vdots \\ \frac{\partial^2 V}{\partial\overline{\beta}_{\overline{V}}\partial\overline{\alpha}_1} & \cdots & \frac{\partial^2 V}{\partial\overline{\beta}_{\overline{V}}\partial\overline{\alpha}_{\overline{U}}} & \frac{\partial^2 V}{\partial\overline{\beta}_{\overline{V}}\partial\overline{\beta}_1} & \cdots & \frac{\partial^2 V}{\partial\overline{\beta}_{\overline{V}}\partial\overline{\beta}_{\overline{V}}} \end{array}\right] \tag{17}$$

which is consistent with the Rayleigh-Ritz procedure. Performing these operations, one obtains Equation 17 in the following expanded form:

$$\begin{aligned} \left[\overline{K}_a\right] = 2\pi\int_r \Big(& K1\cdot\{\dot{u}\}\cdot\{\dot{u}\}^T + K2\{\ddot{u}\}\cdot\{\ddot{u}\}^T + K3\left[\{\dot{u}\}\cdot\{\ddot{u}\}^T + \{\ddot{u}\}\cdot\{\dot{u}\}^T\right] \\ & + K4\left[\{v\}\cdot\{\dot{v}\}^T + \{\dot{v}\}\cdot\{v\}^T\right] + K5\{v\}\cdot\{v\}^T + K6\{\dot{v}\}\cdot\{\dot{v}\}^T \\ & + K7\{\ddot{v}\}\cdot\{\ddot{v}\}^T + K8\left[\{\dot{v}\}\cdot\{\ddot{v}\}^T + \{\ddot{v}\}\cdot\{\dot{v}\}^T\right] \\ & + K9\left[\{v\}\cdot\{\dot{u}\}^T + \{\dot{u}\}\cdot\{v\}^T\right] + K10\left[\{\dot{v}\}\cdot\{\dot{u}\}^T + \{\dot{u}\}\cdot\{\dot{v}\}^T\right] \\ & + K11\left[\{\ddot{v}\}\cdot\{\dot{u}\}^T + \{\dot{u}\}\cdot\{\ddot{v}\}^T\right] + K12\left[\{\dot{v}\}\cdot\{\ddot{u}\}^T + \{\ddot{u}\}\cdot\{\dot{v}\}^T\right] \\ & + K13\left[\{\ddot{v}\}\cdot\{\ddot{u}\}^T + \{\ddot{u}\}\cdot\{\ddot{v}\}^T\right]\Big) r_1\, d\phi \end{aligned} \tag{18}$$

in which

$$\{u\} = \begin{bmatrix} u_1(\xi) \\ \vdots \\ u_{\bar{U}}(\xi) \\ \hline 0_1 \\ \vdots \\ 0_{\bar{V}} \end{bmatrix} \qquad \{v\} = \begin{bmatrix} 0_1 \\ \vdots \\ 0_{\bar{U}} \\ \hline v_1(\xi) \\ \vdots \\ v_{\bar{V}}(\xi) \end{bmatrix}$$

and

$$\{\dot{}\} \equiv \frac{1}{r_1}\frac{d}{d\phi}\{\ \}$$

The form of the coefficients K1 through K13 may be found in Reference 1.

To make the above equation convenient for digital coding two approximations were introduced. The quantities t, C_{11}, C_{12} and C_{22} were assumed to be linear functions of ξ, and C_{33}, C_{34} and C_{44} were assumed cubic functions of ξ. In addition only the membrane component of the initial meridional stress N^o_ϕ was considered. This is a reasonable first order approximation except in very localized areas where bending stresses predominate. The computation of N^o_ϕ therefore simply involves the following integration

$$N^o_\phi = \frac{1}{r \sin\phi}\left[\int p\, r\, dr + C\right]$$

where C is a constant and p represents the pressure distribution acting on the shell structure.

The shell mass matrix associated with the generalized coordinates $\bar{\alpha}_k$, $\bar{\beta}_\ell$ is derived by operating on the expression for the kinetic energy T. For each shell component, the mass matrix is defined by

$$p^2\left[\bar{M}_a\right]_{((\bar{U}+\bar{V})\times(\bar{U}+\bar{V}))} = \left[\begin{array}{ccc|ccc} \frac{\partial^2 T}{\partial\bar{\alpha}_1\partial\bar{\alpha}_1} & \cdots & \frac{\partial^2 T}{\partial\bar{\alpha}_1\partial\bar{\alpha}_{\bar{U}}} & & & \\ \vdots & & \vdots & & 0 & \\ \frac{\partial^2 T}{\partial\bar{\alpha}_{\bar{U}}\partial\bar{\alpha}_1} & \cdots & \frac{\partial^2 T}{\partial\bar{\alpha}_{\bar{U}}\partial\bar{\alpha}_{\bar{U}}} & & & \\ \hline & & & \frac{\partial^2 T}{\partial\bar{\beta}_1\partial\bar{\beta}_1} & \cdots & \frac{\partial^2 T}{\partial\bar{\beta}_1\partial\bar{\beta}_{\bar{V}}} \\ & 0 & & \vdots & & \vdots \\ & & & \frac{\partial^2 T}{\partial\bar{\beta}_{\bar{V}}\partial\bar{\beta}_1} & \cdots & \frac{\partial^2 T}{\partial\bar{\beta}_{\bar{V}}\partial\bar{\beta}_{\bar{V}}} \end{array}\right] \qquad (19)$$

After substitution of Equations 2 to 4 into the kinetic energy expression in Equation 19, the mass matrix assumes the form (Reference 7)

$$M_a = 2\pi\gamma_a \int_t r\left(\{u\}\cdot\{u\}^T + \{v\}\cdot\{v\}^T\right) ds \qquad (20)$$

where γ_a is the shell mass density. Consistent with the matrix formulation, the integration of Equations 18 and 19 is performed using a sixteen point Gaussian (Reference 8) weighted matrix integration scheme.

4.0 FLUID COMPONENT MASS MATRIX

In addition to the mass and stiffness matrices for the shell components, the inertial effects due to the presence of liquid propellants in the vehicle fuel tanks must be considered. The linear analytical model does not include, however, the effective fluid stiffness caused by changes in the fluid head during shell distortions as this is a higher order nonlinear effect.

The general fluid component b is enclosed by three shell components, consisting of conical and ellipsoidal shells of revolution. For a typical fluid component, as shown in Figure 5, the tank is divided into three shells in which the upper bulkhead is referred to as shell a1, the tank wall as shell a2, and the lower bulkhead as shell a3.

The fluid motions are a function of the generalized displacements for shell components, a1, a2 and a3. For the $u_k(\xi)$ or $v_\ell(\xi)$ of each shell element defined by Equation 4 there is an associated fluid motion $\hat{u}_m(x)$ and $\hat{v}_m(x, \hat{r})$, where $1 \le m \le \overline{W}$ and $\overline{W} = (\overline{U}+\overline{V})_{a1} + (\overline{U}+\overline{V})_{a2} + (\overline{U}+\overline{V})_{a3}$. $\hat{u}_m(x)$ is the fluid displacement parallel to the x-axis (longitudinal axis of the vehicle) associated with the tank shell generalized displacement m. $\hat{v}_m(x, \hat{r})$ is the fluid displacement parallel to the r-axis (radial axis of the vehicle) associated with the tank shell generalized displacement m.

The general form of the fluid mass matrix consistent with the fluid displacements may be expressed as (Reference 7)

$$\left[\overline{M}_b\right]_{(\overline{W}\times\overline{W})} = 2\pi\gamma_b \int_{-L_{a3}}^{H} \int_0^r \hat{r}\left(\left\{\hat{u}(x)\right\}\left\{\hat{u}(x)\right\}^T + \left\{\hat{v}(x,\hat{r})\right\}\left\{\hat{v}(x,\hat{r})\right\}^T\right) d\hat{r}\, dx \qquad (21)$$

where

$$\left\{\hat{u}(x)\right\} \equiv \begin{bmatrix} \hat{u}_1(x) \\ \vdots \\ \hat{u}_{\overline{W}}(x) \end{bmatrix}, \quad \left\{\hat{v}(x\hat{r})\right\} \equiv \begin{bmatrix} \hat{v}_1(x,\hat{r}) \\ \vdots \\ \hat{v}_{\overline{W}}(x,\hat{r}) \end{bmatrix} \qquad (22)$$

γ_b is the fluid mass density and matrix $\overline{M}_b$ is of order $\overline{W}$.

The fluid motion $\hat{u}_m(x)$ is assumed independent of location $\hat{r}$ and is obtained by treating the fluid as incompressible and inviscid. From these assumptions, $\hat{u}_m(x)$ is equal to the change in volume below a given location x divided by the corresponding tank cross-sectional area. Thus (see Figure 5)

$$\left\{\hat{u}(x)\right\} = -\frac{2}{r^2} \int_{-L_{a3}}^{x} r\left(\cot\phi \left\{\overline{u(\xi)}\right\}_b + \left\{\overline{v(\xi)}\right\}_b\right) dx \qquad (23)$$

where

$$\left\{\overline{u(\xi)}\right\}_b^T = \left[u_1(\xi)\cdots u_{\overline{U}_1}(\xi), 0_1\cdots 0_{\overline{V}_1}, u_1(\xi)\cdots u_{\overline{U}_2}(\xi), 0_1\cdots 0_{\overline{V}_2}, u_1(\xi)\cdots u_{\overline{U}_3}(\xi), 0_1\cdots 0_{\overline{V}_3}\right]_{(\overline{W}\times 1)}$$

and

$$\left\{\overline{v(\xi)}\right\}_b^T = \left[0_1\cdots 0_{\overline{U}_1}, v_1(\xi)\cdots v_{\overline{V}_1}(\xi), 0_1\cdots 0_{\overline{U}_2}, v_1(\xi)\cdots v_{\overline{V}_2}(\xi), 0_1\cdots 0_{\overline{U}_3}, v_1(\xi)\cdots v_{\overline{V}_3}(\xi)\right]_{(\overline{W}\times 1)} \quad (24)$$

Fluid sloshing motions which disturb the planar character of the assumed longitudinal motion are beyond the scope of this treatment, but may be superimposed as generalized sloshing modes independent of the shell distortions.

Consistent with the assumed longitudinal fluid motion $\hat{u}_k(x)$ and the axisymmetric nature of the linear model, the radial fluid motion $\hat{v}_k(x, \hat{r})$ varies linearly with space coordinate $\hat{r}$. At a particular longitudinal location x, the radial fluid motion is a function of the radial motion of the adjacent tank shell boundary and of the longitudinal fluid motion. Thus

$$\left\{\hat{v}(x, \hat{r})\right\} = \frac{\hat{r}}{r}\left(\cot\phi\left\{u(\xi)\right\}_b + \left\{v(\xi)\right\}_b - \cot\phi\left\{\hat{u}(x)\right\}\right) \quad (25)$$

Upon substituting Equations 23 and 25 into Equation 21 and integrating with respect to r, one obtains

$$\overline{M}_b = \pi\gamma_b \int_{-L_{a3}}^{H}\left(\frac{4}{r^2}\left\{\frac{r^2}{2}\hat{u}(x)\right\}\left\{\frac{r^2}{2}\hat{u}(x)\right\}^T + \frac{1}{2}\left\{r\hat{v}(x, r)\right\}\left\{r\hat{v}(x, r)\right\}^T\right)dx \quad (26)$$

where

$$\left\{\frac{r^2}{2}\hat{u}(x)\right\} = -\int_{-L_{a3}}^{x} r\left(\cot\phi\left\{\overline{u(\xi)}\right\}_b + \left\{\overline{v(\xi)}\right\}_b\right)dx$$

and

$$\left\{r\hat{v}(x, r)\right\} = r\cot\phi\left\{\overline{u(\xi)}\right\}_b + r\left\{\overline{v(\xi)}\right\}_b - r\cot\phi\left\{\hat{u}(x)\right\} \quad (27)$$

The detailed expressions developed for evaluating Equation 26 for the typical cases are given in Reference 1. Unlike the formulation for the shell stiffness and mass matrices, Equation 26 for the fluid mass matrix involves a double integration. For this computation, a double Lagrangian (Reference 9) weighted matrix integration scheme was found most suitable. This technique employs two eleven-point Lagrangian weighting matrices in sequence to provide a twenty-two point approximation.

5.0 LAUNCH VEHICLE COORDINATE SYSTEMS

The matrices for the shell and fluid components are derived in Sections 3.0 and 4.0 respectively, using a system of generalized coordinate displacements (local coordinates), as

given by Equations 2 to 4 to describe the shell distortion. These equations may be written in matrix notation in the following form:

$$u(\xi) = \bar{a}_k \quad A \quad \xi = \xi \quad A^T \quad \bar{a}_k \tag{28}$$

and

$$v(\xi) = \bar{\beta}_\ell \quad B \quad \xi = \xi \quad B^T \quad \bar{\beta}_\ell \tag{29}$$

where

$$\begin{aligned} \bar{a}_k &= \{\bar{a}_1 \ldots \bar{a}_U\} \\ \bar{\beta}_\ell &= \{\bar{\beta}_1 \ldots \bar{\beta}_V\} \\ \xi &= \{1 (\xi) (\xi)^2 \ldots (\xi)^{10}\} \end{aligned} \tag{30}$$

In order to work with reference to a space frame, however, it is necessary to transform the generalized coordinates to space coordinates designated as system coordinates. The system coordinates represent displacement and rotations at specific points on each shell component and thus facilitate representing attachments of adjacent shell components, connections of spring-mass components, and applications of force inputs at arbitrary stations along the vehicle.

For each shell component, system coordinates are provided to represent displacements in the longitudinal and radial directions at equally spaced intervals along the shell meridian, and tangential rotations at the edges of the shell. Longitudinal displacements $\{u(\xi_i)\}$ at locations $\xi_i = (U - i)/(U - 1)$, where $i = 1, 2, \ldots, U$ are expressed (using Equation 28) as

$$\{u(\xi_1)\}_{(U \times 1)} = U \quad A^T \quad \bar{a}_k \tag{31}$$

where

$$[U] = \begin{bmatrix} 1_1 & \xi_1 \ldots (\xi_1)^{10} \\ \vdots & \vdots \quad \vdots \\ 1_U & \xi_U \ldots (\xi_U)^{10} \end{bmatrix} \tag{32}$$

Longitudinal displacements $\{v(\xi_j)\}$ at locations $\xi_j = (V - j)/(V - i)$, where $j = 1, 2, \ldots, V$, are similarly expressed (using Equation 29) as

$$\{v(\xi_j)\}_{(V \times 1)} = V \quad B^T \quad \bar{\beta}_\ell \tag{33}$$

where

$$V = \begin{bmatrix} 1_1 & \xi_1 \cdots (\xi_1)^{10} \\ \vdots & \vdots \\ 1_V & \xi_V \cdots (\xi_V)^{10} \end{bmatrix} \tag{34}$$

The scalar quantities U and V are prescribed constants which define the number of system coordinate point displacements to be provided in the longitudinal and radial directions, respectively, for a given shell component. These are related to U and V, as discussed in the end of this section. The shell rotations, $\rho 1$ and $\rho 2$, are evaluated at $\xi = 1$ and 0, respectively, and can be shown to have the following form:

$$\begin{bmatrix} \rho 1 \\ \rho 2 \end{bmatrix} = D_1 \; A^T \; \bar{\alpha} + D_2 \; B^T \; \{\bar{\beta}\} \tag{35}$$

where

$$D_1 = D_1 \begin{bmatrix} 0 & 1 & 2 \cdots 9 & 10 \\ 0 & 1 & 0 \cdots 0 & 0 \end{bmatrix}_{(2 \times 11)}$$

$$D_2 = D_2 \begin{bmatrix} 0 & 1 & 2 \cdots 9 & 10 \\ 0 & 1 & 0 \cdots 0 & 0 \end{bmatrix}_{(2 \times 11)} \tag{36}$$

and D_1 and D_2 are constants which depend on the geometry of the shell (see Reference 1).

The total vector of system coordinate displacements for shell component "a" is defined from Equations 31, 33 and 35 as

$$\{a_a\}_{(\bar{U}+\bar{V})\times 1} = \begin{bmatrix} u(\xi_i) \\ v(\xi_j) \\ \rho 1 \\ \rho 2 \end{bmatrix} \tag{37}$$

The local coordinate displacements for shell component "a" are related to the system coordinate displacements by the transformation $[T_a]$ as follows:

Consolidating the arrangement of local coordinate displacements, as defined in Equations 28 to 30, let

$$\{\bar{a}_a\}_{(\bar{U}+\bar{V})\times 1} = \begin{bmatrix} \bar{\alpha}_k \\ \bar{\beta}_\ell \end{bmatrix} \tag{38}$$

Consistent with the system coordinate displacement vector $\{\alpha_a\}$ given by Equations 31, 33 and 35, the transformation matrix $[T_a]$ which relates local to system coordinates, is defined by the equation

$$\alpha_a = T_a^{-1} \bar{\alpha}_a \tag{39}$$

where, in general,

$$[T_a]^{-1} = \left[\begin{array}{c|c} U & 0 \\ \hline 0 & V \\ \hline D_1 & D_2 \end{array}\right] \left[\begin{array}{c|c} A^T & 0 \\ \hline 0 & B^T \end{array}\right] \tag{40}$$

Thus

$$\bar{\alpha}_a = T_a \alpha_a \tag{41}$$

It is apparent that computation of the matrix T_a requires inversion of the matrix T_a^{-1}, which must therefore be nonsingular, square, and of order $(\bar{U} + \bar{V})$. This will require for some components modification of the general Equation 40, as discussed in Reference 1. Special attention must be given the scalar quantities U, V, $\bar{U}$, $\bar{V}$ and the matrices **A**, **B**, D_1, D_2 to satisfy the above conditions consistent with the shell component boundary conditions. The matrix T_a^{-1} may also be poorly conditioned and difficult to invert accurately if $\bar{U}$ and/or $\bar{V}$ are equal to or greater than six. For these cases it is recommended that Shifted Chebyshev Polynomial Coefficients (Reference 10) be used for the **A** and **B** matrices to improve the accuracy of the matrix T_a calculation.

As illustrated in Figure 5, and discussed in Section 4.0, the distortion of each fluid component "b" is a function of the distortion of the three enclosing shell components a1, a2 and a3. The local to system coordinate transformation matrix T_b for the fluid component is thus obtained as a combination of the shell component transformations T_a for a = a1, a2 and a3, as follows:

Consolidating the arrangement of local coordinate displacements, as defined by Equations 24 and 38, let

$$\bar{\alpha}_b = \begin{bmatrix} \bar{\alpha}_{a1} \\ \bar{\alpha}_{a2} \\ \bar{\alpha}_{a3} \end{bmatrix} \tag{42}$$

Consistent with Equation 37, let the consolidated vector of system coordinate displacements be

$$\alpha_b = \begin{bmatrix} \alpha_{a1} \\ \alpha_{a2} \\ \alpha_{a3} \end{bmatrix} \tag{43}$$

Corresponding to Equations 41, 42, and 43, the transformation matrix T_b is defined by

$$\bar{a}_b = T_b \; a_b \tag{44}$$

where

$$T_b = \begin{bmatrix} T_{a1} & 0 & 0 \\ 0 & T_{a2} & 0 \\ 0 & 0 & T_{a3} \end{bmatrix}_{(\bar{W} \times \bar{W})} \tag{45}$$

6.0 LAUNCH VEHCILE STIFFNESS AND MASS MATRIX SYNTHESIS

In order to construct the total vehicle stiffness and mass matrices referenced to a common coordinate system, the individual component stiffness and mass matrices are expressed in terms of the system coordinates using transformations developed in the previous section. For each shell and fluid component e, the matrices, transformed (Reference 4) to system coordinates, become

$$K_e = T_e^T \; \bar{K}_e \; T_e \qquad \text{Note: } \bar{K}_e \equiv 0 \text{ for fluid components, i.e., for } e = b. \tag{46}$$

and

$$M_e = T_e^T \; \bar{M}_e \; T_e$$

where T_e is the transformation matrix defined in Equation 41 for shell components and in Equation 44 for fluid components. $\bar{K}_e$ and $\bar{M}_e$ are the stiffness and mass matrices related to the local coordinate system. The stiffness and mass matrices for the spring-mass components do not undergo the transformation Equation 46, since they can be provided initially in terms of the system coordinate displacements.

The total system stiffness and mass matrices are synthesized by first expanding each of the component matrices (Equation 46) into an enlarged matrix which is of the same order as the total system matrix and which is related to the set of system coordinates for the total vehicle, as shown in Figure 1b. These matrices are then superimposed to arrive at the total system characteristics.

These operations can be readily accomplished by introducing the transformation matrix Δ_e relating the total system displacements a to the component e system displacements a_e (contained in $\{a\}$) as defined by

$$a_e = \Delta_e \; a \tag{47}$$

in which the elements of Δ_e are either unity or zero (see Reference 1).

The total system stiffness and mass matrices can then be formed as follows:

$$[K]_{(N_X \times N_C)} = \sum_{a=1}^{N_S} \Delta_a^T \; K_a \; \Delta_a + \sum_{c=1}^{N_M} \Delta_c^T \; K_c \; \Delta_c \qquad (48)$$

and

$$[M]_{(N_C \times N_C)} = \sum_{a=1}^{N_S} \Delta_a^T \; M_a \; \Delta_a + \sum_{b=1}^{N_F} \Delta_b^T \; M_b \; \Delta_b + \sum_{c=1}^{N_M} \Delta_c^T \; M_c \; \Delta_c \qquad (49)$$

in which N_C, N_S, N_F and N_M are the total number of system coordinates, shell components, fluid components and spring-mass components, respectively. The matrices K_a, M_a and M_b are, respectively, the stiffness and mass matrices for the shell components and the mass matrix for the fluid components, as defined by Equation 46.

The superposition technique assures displacement compatibility and force equilibrium at the joints between components. Displacement boundary conditions are imposed on the total stiffness and mass matrix by removing appropriate rows and columns of coefficients corresponding to points on the vehicle and its support which are rigidly restrained from motion.

7.0 DYNAMIC RESPONSE EQUATIONS

The total stiffness and mass matrices are used for computation of the natural frequencies and mode shapes from the eigenvalue equation

$$K \quad \alpha \quad - p^2 \; M \quad \alpha \quad = 0 \qquad (50)$$

in which p is the circular frequency of the launch vehicle and α is the modal vector whose elements are the longitudinal, radial and rotational system coordinate displacements. This equation is solved to obtain the natural frequencies p_t and the mode shapes for all modes, t, which are arranged in a square modal matrix **A**. Each column, A_t, (of **A**,) is the mode t displacement vector with system coordinate elements, whereas each row, A_s, of **A**, is the system coordinate s displacement vector with natural mode elements.

The steady-state response due to simple harmonic loads of frequency ω is determined using a standard modal technique. The elements of the load vector **P** represent axisymmetric forces (longitudinal and radial) or moments, depending on whether the associated coordinate is a displacement or a rotation. The displacement response vector **R** is expressed as the linear superposition of the individual model responses based on an assumed modal damping factor η_t which is the ratio of the actual damping to the critical damping for each mode and has the form: (Reference 4)

$$\{R\} = \{\overline{R} \sin (\omega t - \overline{\delta})\}$$

where

$$\left\{\bar{R}^2\right\} = \left\{\left(A\left\{\frac{Q_t \sin\delta_t}{m_t\left(p_t^2 z_t\right)}\right\}\right)^2 + \left(A\left\{\frac{Q_t \cos\delta_t}{m_t\left(p_t^2 z_t\right)}\right\}\right)^2\right\} \tag{51}$$

$$\left\{\bar{\delta}\right\} = \left\{\tan^{-1}\left(\frac{A_s\left\{\frac{Q_t \sin\delta_t}{m_t\left(p_t^2 z_t\right)}\right\}}{A_s\left\{\frac{Q_t \cos\delta_t}{m_t\left(p_t^2 z_t\right)}\right\}}\right)\right\} \tag{52}$$

$$\begin{aligned} Q_t &= A_t^T \quad P \\ m_t &= A_t^T \quad M \quad A_t \\ p_t^2 z_t &= \left[\left(p_t^2 - \omega^2\right)^2 + 4 p_t^2 \eta_t^2 \omega^2\right]^{1/2} \end{aligned} \tag{53}$$

and

$$\delta_t = \tan^{-1}\frac{2\eta_t\left(\frac{p_t}{\omega}\right)}{\left(\frac{p_t}{\omega}\right)^2 - 1}$$

In these equations, $\delta_t = \pi$ when $p_t = 0$, and $\delta_t = 0$ when $p_t \neq 0$, $\omega = 0$. $\{\bar{R}\}$ and $\{\bar{\delta}\}$ represent, respectively, the vectors of steady-state displacement amplitude and the phase angle by which the forcing function leads (+) or lags (-) the response.

The internal forces (or moments) S_a acting at each point along the vehicle on each shell component a are obtained from the equation:

$$\left\{S_a\right\}_{\left((\bar{U}+\bar{V})\times 1\right)} = \left\{\bar{S}\sin(\omega t - \delta)\right\} \tag{54}$$

where

$$\left\{\bar{S}^2\right\}_{\left((\bar{U}+\bar{V})\times 1\right)} = \left\{\left(K_a \quad \Delta_a \left\{\bar{R}\sin\bar{\bar{\delta}}\right\}\right)^2 + \left(K_a \quad \Delta_a \left\{\bar{R}\cos\bar{\bar{\delta}}\right\}\right)^2\right\}$$

$$\left\{\bar{\bar{\delta}}\right\}_{\left((\bar{U}+\bar{V})\times 1\right)} = \left\{\tan^{-1}\left(\frac{K_s \quad \Delta_a \left\{\bar{R}\sin\bar{\delta}\right\}}{K_s \quad \Delta_a \left\{\bar{R}\cos\bar{\delta}\right\}}\right)\right\} \tag{55}$$

$\{\bar{S}\}$ and $\{\bar{\bar{\delta}}\}$ represent, respectively, the amplitude and phase angle of the internal forces. K_s is row s (s = 1, 2, ..., $(\bar{U} + \bar{V})_a$) of the shell element stiffness matrix K_a. $\{\bar{R}\}$ and $\{\bar{\delta}\}$ are obtained from Equation 52. In the solution of Equation 50, the storage capacity of the computer limits the size of the matrices **K** and **M**. This restriction may be relaxed, in an approximate fashion, by utilizing a reduction technique described in Reference 11. In this approach the inertia force at coordinates which exhibit a high frequency are carried as structurally equivalent forces (Reference 12) at the other coordinate points. This assumption, which has only a small effect on the significant low frequency modes, enables the matrices to be reduced to a size for which the computer can obtain the eigenvalue solution.

8.0 NUMERICAL EXAMPLE

The natural frequency solution for a typical one-stage launch vehicle (see Figure 6) is presented for illustration and also to contrast the solution with results obtained from a lumped spring-mass model.

For simplicity it is assumed that all structural components are constructed of aluminum. Two of the shell sections have been given orthotropic properties as noted in Figure 6. The physical model is subdivided into a consistent set of shell, fluid and spring-mass components as shown in Figure 7a. The vehicle is represented by eleven shell components, two fluid components, and four spring-mass components to account for the payload, engine and equipment. Thirty-three displacement coordinate locations are then selected and given identification numbers. The vehicle is assumed to be unsupported.

The contrasting lumped spring-mass model is illustrated in Figure 7b. The vehicle behavior is described by 16 masses connected by simple springs representing tank, bulkhead and interstage flexibilities in the manner discussed in Reference 3.

Solutions for the lowest natural frequency modes are tabulated in Table 1. It is noted that several significant modes which result from the shell model could not have been simulated by the spring-mass model. These modes represent large tank distortions which do not cause significant changes in the center of gravity of the contained fluid. The frequencies which do correspond are in general lower in the shell model due to the presence of more degrees of freedom which provide more flexibility.

Table 1. Natural Frequency Solutions

Mode	Description	Frequency (cps)	
		Shell Model	Spring-Mass Model
1	Rigid-Body	0	0
2	Pogo-Mode	37.7	37.1
3	Payload Mode	60.0	59.7
4	Payload Upper-Tank Mode	83.1	---
5	Engine Mode	114.8	138.3
6	Engine Lower-Tank Mode	177.2	---
7	Engine Upper-Tank Mode	225.5	251.4

REFERENCES

1. Archer, John S., and Rubin, C. P., Improved Analytic Longitudinal Response Analysis for Axisymmetric Launch Vehicles, Vol. I, TRW Systems, May 1965.

2. Rubin, C. P., and Wang, T. T., Improved Analytic Longitudinal Response Analysis for Axisymmetric Launch Vehicles, Vol. II, TRW Systems, May 1965.

3. Wood, J. D., Survey on Missile Structural Dynamics, EM11-11, TRW Systems, 1 June 1961.

4. Timoshenko, S., and Gere, J. M., Theory of Elastic Stability, 2nd edition, McGraw-Hill Book Co., New York, 1961.

5. Flügge, W., "Stresses in Shells," Springer-Verlag, pp. 18-24, 97, 355-359, 1960.

6. Thielemann, W. F., "New Developments in the Nonlinear Theories of the Buckling of Thin Cylindrical Shells," Proc. of the Durant Centennial Conference, Pergamon Press, New York, 1960.

7. Archer, John S., "Consistent Matrix Formulations for Structural Analysis Using Influence-Coefficient Techniques," Preprint No. 64-488, Am. Inst. Aeron. and Astronaut, June - July 1964.

8. Handbook of Mathematical Functions with Formulas, Graphs and Mathematical Tables, U. S. Dept. of Commerce, National Bureau of Standards, Applied Mathematic Series, 1964.

9. Tables of Lagrangian Interpolation Coefficients, National Bureau of Standards, Computation Laboratories, Columbia University Press, New York.

10. Lanczos, Cornelius, Applied Analysis, Prentice-Hall, Inc., p. 516, 1956.

11. Archer, J. S., and Yeh, G. C. K., Successive Reduction of the Order of Matrix Formulation in Dynamic Structural Analysis, TRW Systems, Report No. 7120-6268-RU000, EM15-9, June 1965.

12. Schmitt, A. F., "A Least Squares Matrix Interpolation of Flexibility Influence Coefficients," Journal of the Aeronautical Sciences, Vol. 23, No. 11, p. 980, October 1956.

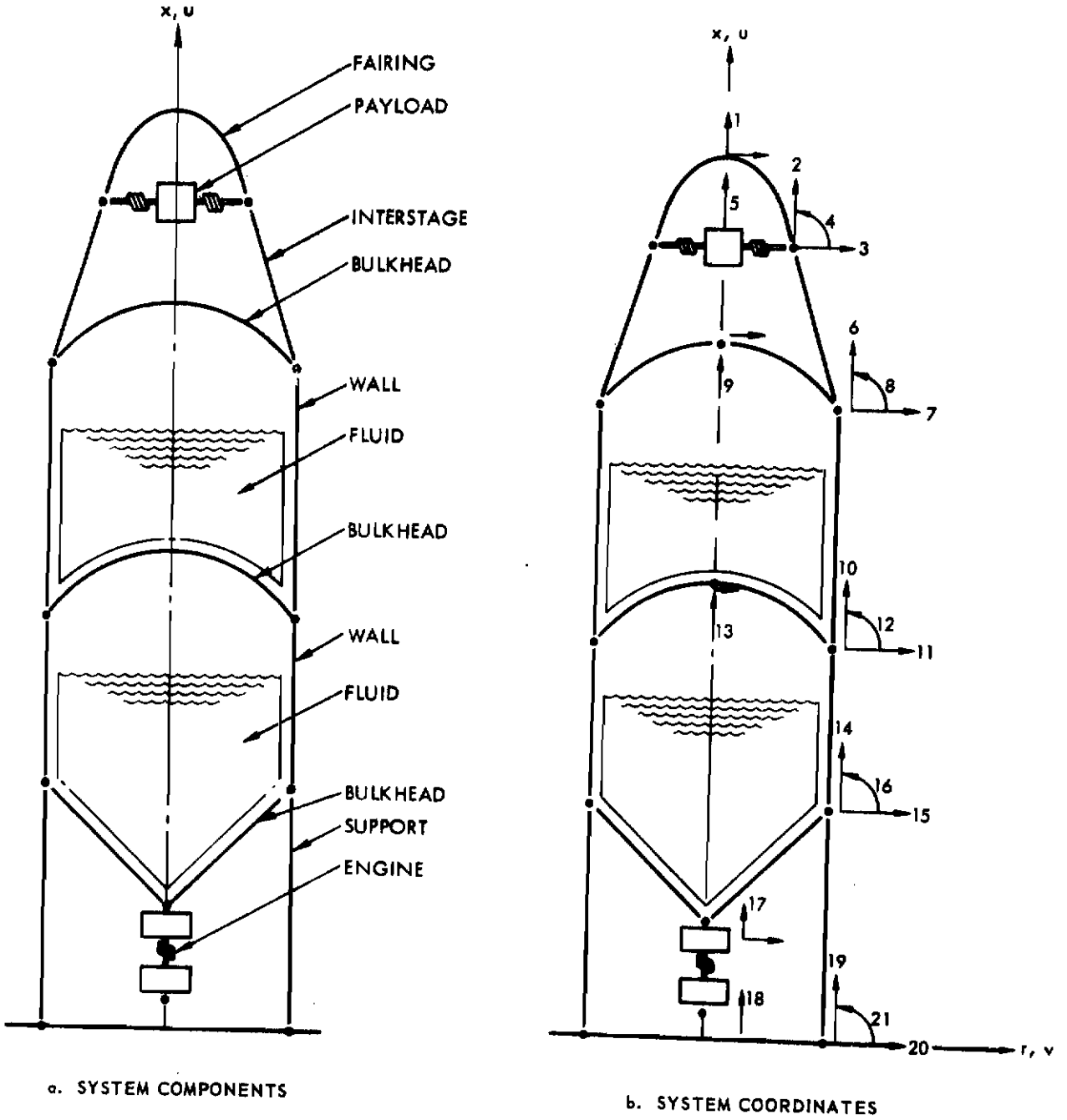

a. SYSTEM COMPONENTS

b. SYSTEM COORDINATES

Figure 1 Launch Vehicle

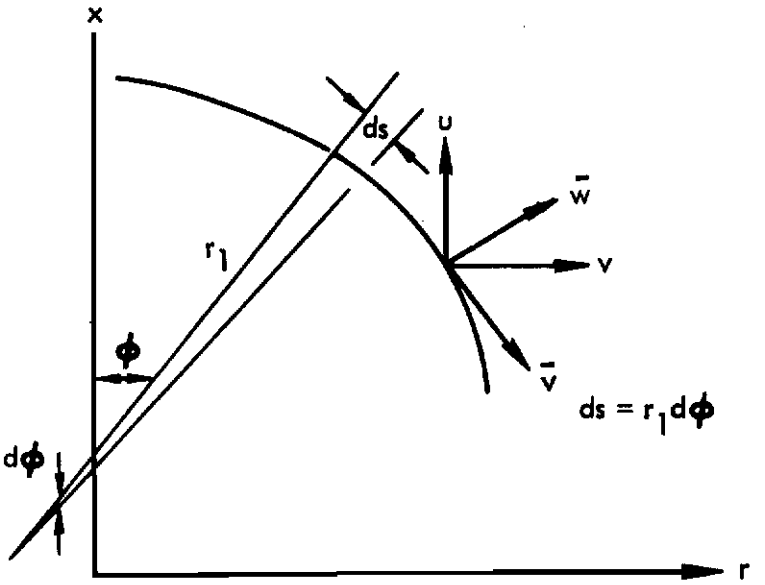

Figure 2 Displacements of Shell of Revolution

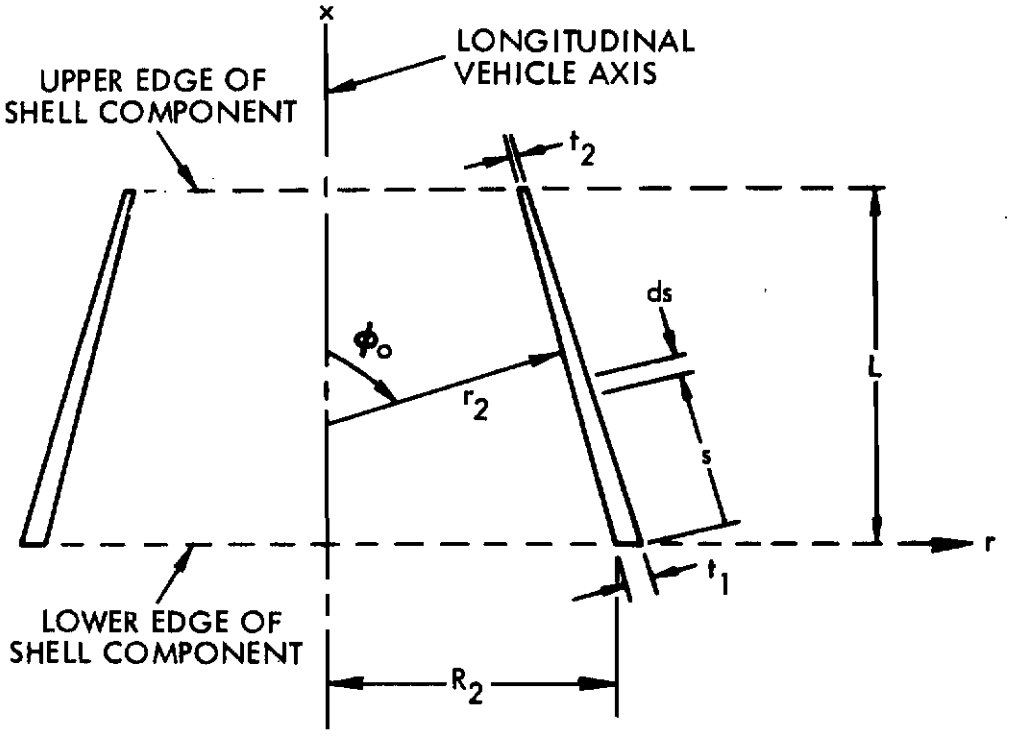

(TRANSVERSE CROSS SECTION THROUGH LONGITUDINAL AXIS)

Figure 3 Conical Shell Component

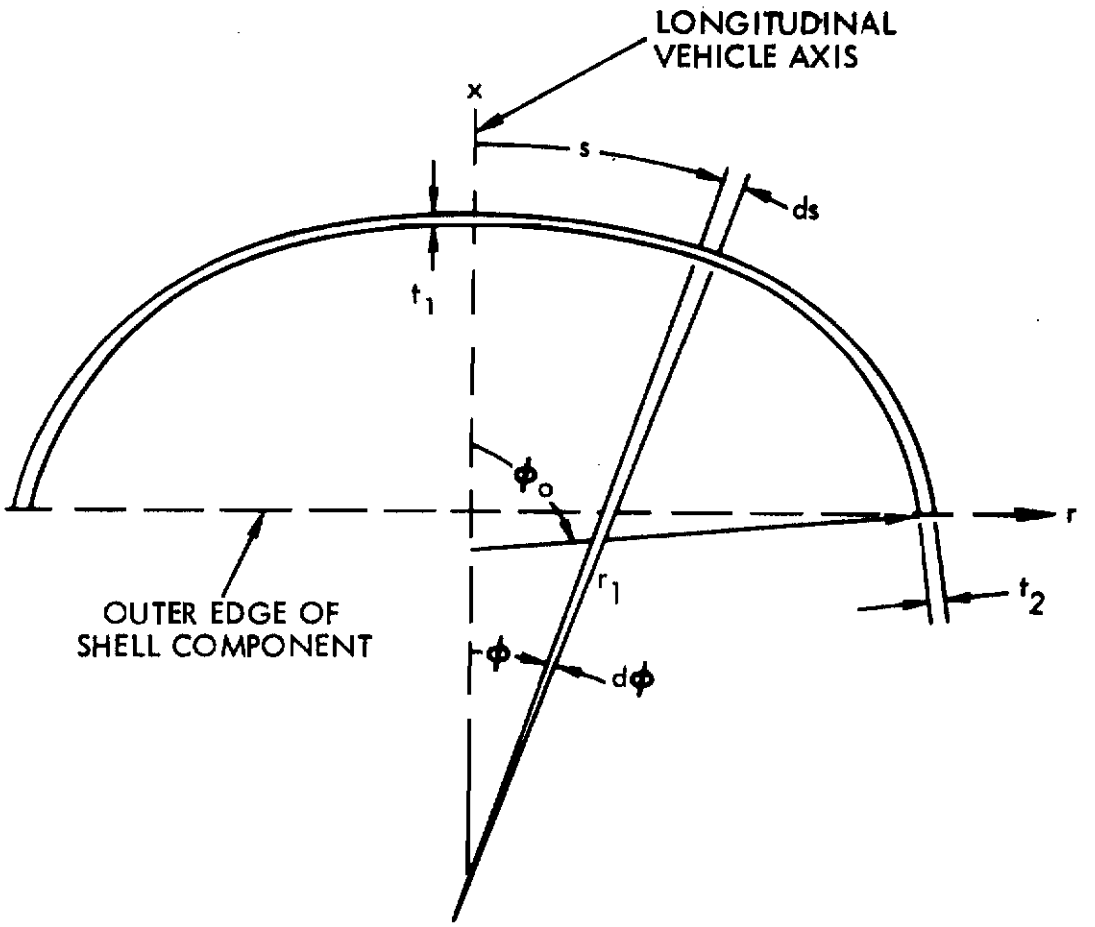

(TRANSVERSE CROSS SECTION THROUGH LONGITUDINAL AXIS)

Figure 4 Ellipsoidal Bulkhead Component

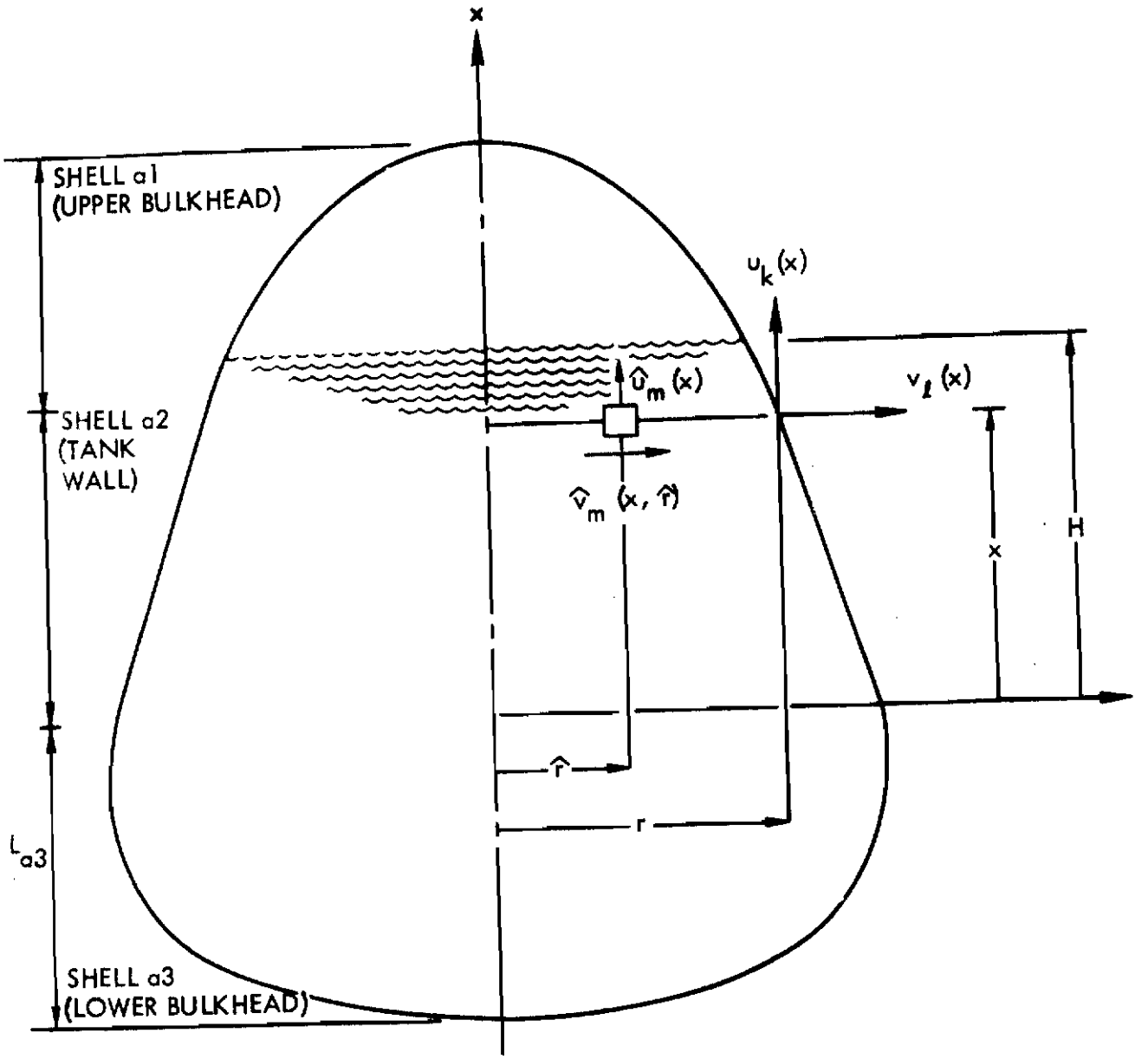

Figure 5 Definition of Fluid Motions

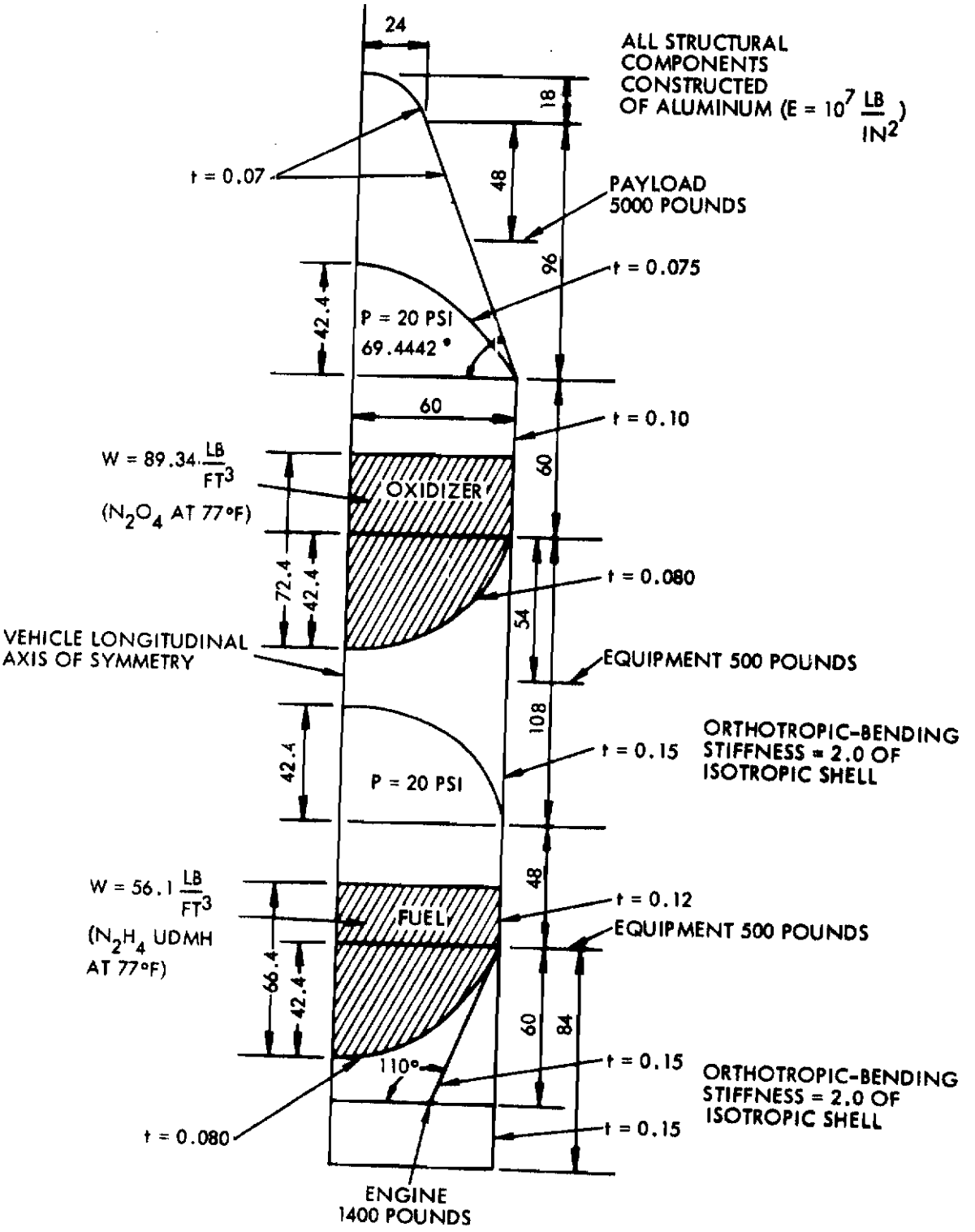

Figure 6 Typical One-Stage Launch Vehicle

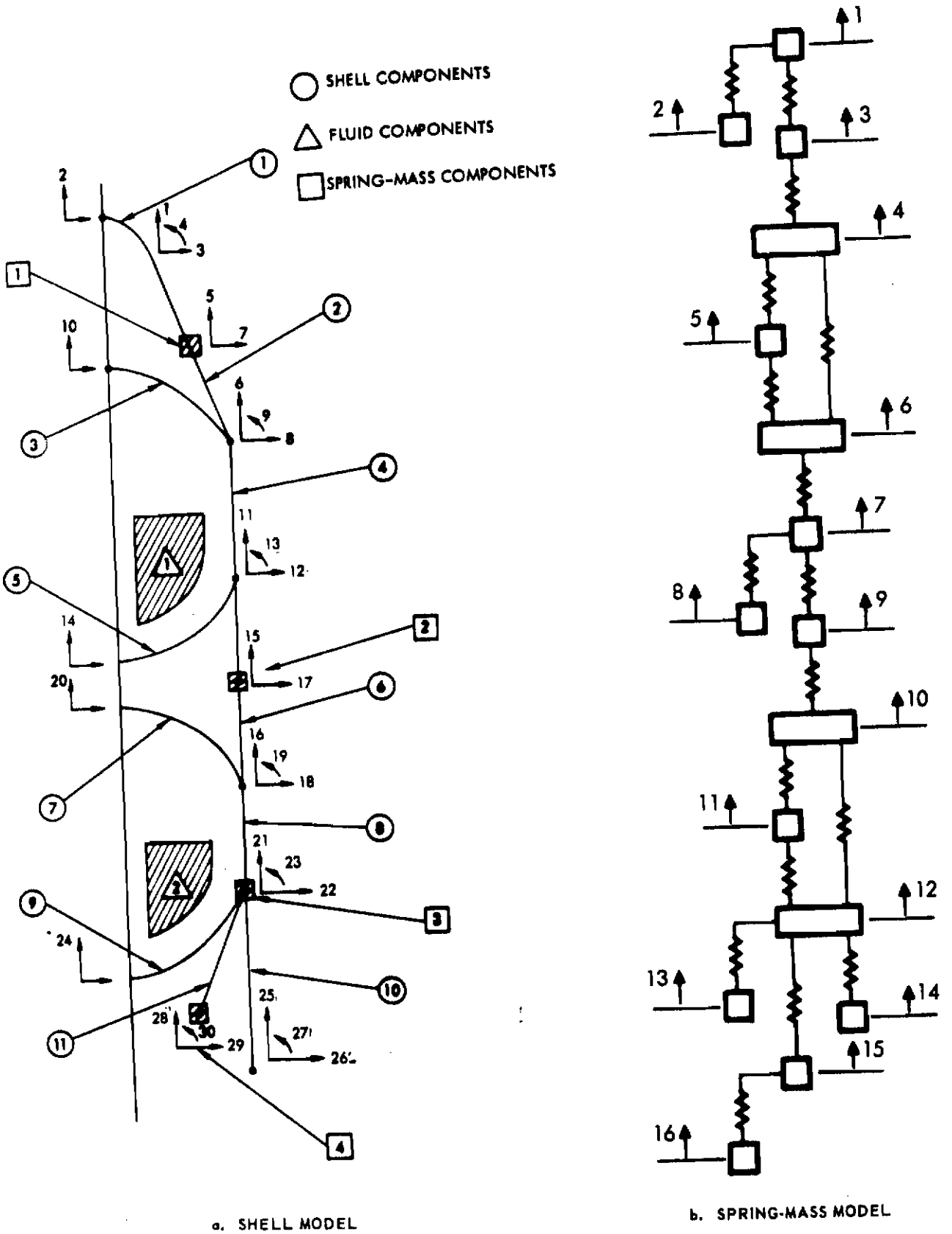

Figure 7 Launch Vehicle Analytical Models